21aE-4

Modification of ITER Equatorial EC Launcher Design enhancing EC H&CD function
電子サイクロトロン波加熱電流駆動性能向上のためのITER水平ECランチャー設計の改良

K. Takahshi, G. Abe, M. Isozaki, R. Ikeda, Y. Oda, K. Sakamoto
髙橋幸司、阿部岩司、磯崎正美、池田亮介、小田靖久、坂本慶司

Japan Atomic Energy Agency
801-1, Mukoyama, Naka, Ibaraki 311-0193, Japan
日本原子力研究開発機構 〒311-0193 那珂市向山801-1

It is expected that a poloidal beam steering from the equatorial launcher (EL) can enhance driven current at the peripheral region of plasma, ρ = 0.4 ~ 0.6. In order to fulfill the task, the baseline design of the ITER equatorial launcher, which has the function of toroidal beam steering, is modified. The modification of millimeter (mm)-wave design to attain the poloidal beam steering with transmission efficiency of 99% has been successfully obtained and the structural design of the launcher components such as blanket shield modules (BSMs), port plug and so on are also modified based on the mm-wave design modification. This modification ensures that mm wave beams from both middle and bottom beam row pass through the same BSM opening and will leads to the neutron shielding potential. The electromagnetic analysis of the modified EL shows that induced force and momentum torque on the modified BSMs are below the mechanical criteria of the support structure of each BSMs.

1. Introduction

An electron cyclotron heating and current drive (EC H&CD) will be an effective tool to achieve steady state and enhanced performance plasma operation and suppression of MHD instabilities such as neoclassical tearing modes (NTMs) and sawteeth [1-3] for a fusion device like ITER. ITER will install the EC H&CD system consisting of twenty-four 170GHz, ≥1MW gyrotrons [4-6], the power supply system to operate the gyrotrons [7], twenty-four transmission lines with the length of 100~150m[8, 9] and one equatorial port and four upper port electron cyclotron launchers [10-12].

The equatorial launcher (EL) was required to have the functionality of 170GHz, 20MW millimeter (mm) wave beam injection into the plasma with toroidal beam steering from 20º to 40º. It consists of a front shield structure configured by several pieces of blanket shield modules (BSMs) and port plug structure installing the mm-wave components, internals shield structure and cooling pipes. The schematic view of the toroidal steering EL is shown in Fig. 1(a). All beams radiated from the waveguides are reflected at the fixed mirror toward the steering mirror and are injected into plasma at a certain toroidal angle set by the movable mirror. Two of three steering mirrors totally inject sixteen beams in the co-direction accessing from center to nearly half of the plasma cross section. The third steering mirror injects eight beams in the counter-direction accessing similar region with the co-injection. It was estimated that driven co-current was 350 kA (ρ=0.4) for 15 MA scenario and 640 kA (ρ=0.4) for 9 MA scenario [13]. However, effective driven current at further off-axis (0.4<ρ<0.6) can not be obtained in this configuration.

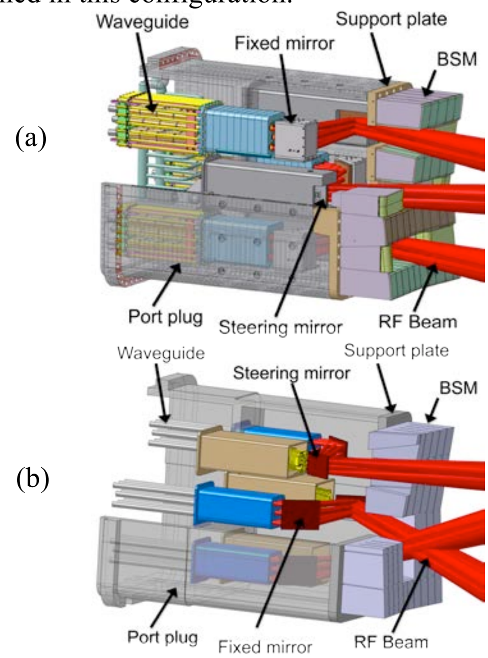

Fig 1 Schematic view of ITER equatorial launcher, (a) toroidal and (b) poloidal beam steering.

In order to drive more current at 0.4<ρ<0.6, the poloidal beam steering functionality has been considered. Toroidal angle of co- and counter-injection is fixed to be 25 º and 20 º, respectively. The counter-injection of beams at the top row and co-injection of beams at the middle and bottom row are configured. It was estimated that driven current at $0.4<\rho<0.6$ for 15 MA and 9 MA scenario with the poloidal steering configuration were 250~400 kA and 480~720 kA, respectively [14].

2. Design of poloidal steering EL

Figure 1(b) shows the schematic view of the poloidal beam steering EL. The configuration of the mm-wave components mostly remains the same as the toroidal steering EL shown in Fig. 1(a). The BSM opening configuration is also modified from horizontal to vertical slots and resulted to two slots. It can be realized that both middle and bottom beam propagate through the same opening. The required steering angle ranges of Top, Middle and Bottom are "$-10 \leq \Theta_P \leq 10$", "$-30 \leq \Theta_P \leq -5$" and "$10 \leq \Theta_P \leq 30$", respectively. Positive and negative sign means the up/downward beam injection.

The mm-wave design is performed by the optimization calculation of mm-wave beam propagation using the optics design code, ZEMAX®, which uses both angular spectrum for near field and Fresnel diffraction for far field. Multi-beams propagated through the free space region in the launcher are superposed and transmission efficiency and power profile of the superposed beams at each aperture are calculated. The design parameters are optimized with the calculation criteria of the mm-wave transmission efficiency between the waveguide and BSM outlet, heat load at both the fixed (M1) and steering (M2) mirrors and beam size at the plasma target.

The optimization process has successfully obtained a transmission efficiency of mm-wave propagation from the waveguides to BSM opening of 99 % assuming propagation of a pure HE_{11} mode wave in the waveguides. Note that the largest degradation of transmission efficiency occurs at the steering mirror (M2) and inside of BSM opening although the degradation is only 0.3 %.

Table I Resulted design parameters

	Resulted design parameters
BSM opening 1 height / width (mm)	415(h) / 240(w)
BSM opening 2 height / width (mm)	415(h) / 240(w)
BSM opening 3 height / width (mm)	580(h) /280(w)
M1 height / width, vertical/horizontal curvature (mm)	365(h) / 460(w), 2155/11645
M2 height / width, vertical/horizontal curvature (mm)	250(h) / 360(w), -3393/20495
Beam duct 1 height and width (mm)	285(h) / 330(w)
Beam duct 2 height and width (mm)	270(h) / 285(w)
Waveguide installtion at horizontal angle (°)	1.39(Beam 3, 8), 1.53(Beam 1, 6), 0.0(Beam 2, 4, 5, 7)
Waveguide installtion at vertical angle (°)	0.0

It was evaluated that peak heat load on M1 and M2 and the beam radius at plasma target were 4.95 MW/m^2 and 3.0 MW/m^2, and 25 cm respectively. The resulted design parameters of the mm-wave design for the top beam row are summarized in Table I.

3. Electromagnetic and nuclear analysis

The induced current on the major disruption with the fast plasma current quench (exponential decay in 16 msec), which was the worst case scenario for the EL was calculated. Then, induced momentum torque on the BSMs in radial, horizontal and vertical component were evaluated to be 60 kN•m, 7 kN•m and 20 kN•m, respectively, which are less than the criteria of the support key (150 kN•m). Maximum momentum toque on the entire EL was also evaluated to be 5.6 MN•m, which was less than the criteria (10 MN•m).

The preliminary result of nuclear analysis indicates that the residual dose rate after shut down at the EL back end was reduced by 20%, compared to that of toroidal steering EL.

5. Conclusion

Millimeter wave design rearrangement of ITER EL is performed by the optimization calculation of mm-wave beam propagation and it is successfully obtained that transmission efficiency of mm-wave propagation from the waveguides to BSM opening is 99 % assuming a pure HE_{11} mode wave propagated in the waveguides. This innovative modification ensures that mm-wave beams at both middle and bottom beam row pass through the same BSM opening. The preliminary result of electromagnetic analysis shows that induced force and momentum torque of the modified BSMs are below the mechanical criteria of the support structure. It is also obtained that maximum momentum toque on the entire poloidal steering EL is reduced by 30%, compared to the toroidal EL design.

References

[1] A. Isayama et al., Nucl. Fusion, **47** (2007) 773.
[2] I.T. Chapman et al., Nucl. Fusion, **52** (2012) 063006
[3] M. Maraschek, Nucl. Fusion **52** (2012) 074007.
[4] Sakamoto K. et al, Nature Phys. **3** (2007) 411.
[5] A. G. Litvak, et al., Conf. Digest of IRMMW, (2006) 8.
[6] B. Piosczyk, et al., Fusion Eng. Design, **66-68**, (2003) 481.
[7] T. Bonicelli, et al., Proc 13th European conference on power elecyronics and applications, 1-10 (2009)
[8] K. Takahash, et al., Proc. 8th International Vacuum Electronics Conference, Kitakyushu, Japan, 2007.
[9] R. W. Callis et al., Fusion Eng. Design, **84**, (2009) 526.
[10] K. Takahashi, et al., Fusion Sci. Technol. **47** (2005) 1.
[11] K. Takahashi, et al., Nucl. Fusion **48** (2008) 054014.
[12] Henderson M.A. et al, Nucl. Fusion **48** (2008) 054013.
[13] D. Farina, et al., Nucl. Fusion **52** (2012) 033005.
[14] D. Farina, et al., Phys. Plasmas **21** (2014) 061504.